



# Simulating Microwave-Heated Diffusion in Zeolite Nanopores

Cristian Blanco<sup>a</sup> and Scott M. Auerbach<sup>a, b, \*</sup>

<sup>a</sup>*Department of Chemistry, University of Massachusetts, Amherst, Massachusetts 01003, USA*

<sup>b</sup>*Department of Chemical Engineering, University of Massachusetts, Amherst, Massachusetts 01003, USA*

We have performed equilibrium molecular dynamics and microwave (MW) heated molecular dynamics simulations to explore how MW heating influences self-diffusion in zeolite nanopores. We have applied these simulations to methanol and/or benzene in de-aluminated Y zeolite. We have found that even under the non-equilibrium conditions of MW heating, center-of-mass motions can be associated with effective temperatures. However, we find that the temperatures controlling kinetic and potential energy distributions are not generally the same in MW-heated systems, with potential temperatures generally exceeding kinetic ones. This finding has a consequence for understanding MW-heated diffusion in zeolites. In particular, when temperatures are sufficiently high that diffusion is not strongly activated, MW-heated diffusivities are equal to equilibrium diffusivities at the same kinetic temperature. On the other hand, when diffusion becomes more strongly activated at lower temperatures, MW-heated diffusivities consistently exceed equilibrium diffusivities at the same kinetic temperature, because the MW-heated potential distributions enable more facile barrier crossing. This result shows that, in general, MW-heated diffusion is more complicated than simply “different components diffusing at different temperatures.” Instead, we advocate the picture involving different components diffusing at different kinetic and potential temperatures.

**Keywords:** Diffusion, zeolites, nanopores, microwaves, energy distributions, steady-states, molecular dynamics.

## 1. INTRODUCTION

Zeolites are nanoporous crystalline aluminosilicates with a rich variety of interesting properties and industrial applications.<sup>1</sup> With over 140 zeolite framework topologies synthetically available—each with its own range of compositions—zeolites offer size-, shape- and electrostatically-selective adsorption, diffusion and reaction up to remarkably high temperatures. Zeolites are widely used as petroleum catalysts, desiccants, ion exchangers and filters, environmentally safe detergents, and as molecular sieves for separating chemical mixtures. It is safe to say that zeolites offer a rich array of nanotechnologies.

The structural and chemical versatility offered by zeolites strongly suggests that other applications lie ahead for these materials. During the past few years, a flurry of interest has emerged in using microwave-heated zeolites in chemical processes, such as catalyst synthesis,<sup>2–4</sup> ion

exchange,<sup>5</sup> reactions<sup>6, 7</sup> and separations.<sup>8, 9</sup> For example, Turner et al.<sup>9</sup> have recently studied the effects of microwave (MW) heating on a binary mixture of cyclohexane and methanol adsorbed in siliceous zeolites FAU and MFI.<sup>10</sup> They found that the effect on sorption selectivity from conventional heating can be reversed by applying MW radiation. Despite this significant research activity, there remains disagreement whether MW-driven systems really behave in ways that are qualitatively different from conventionally heated systems.<sup>2, 11, 12</sup> This disagreement is fueled by the lack of a fundamental, atomistic picture for such MW-driven systems.

In recent work, we explored the nature of energy distributions in MW-driven zeolite systems using non-equilibrium molecular dynamics (MD) techniques.<sup>13, 14</sup> We found that in MW-driven systems, it is possible to maintain various components at statistically different temperatures, suggesting that MW heating may produce novel athermal effects. For example, a MW-heated zeolite containing adsorbed benzene and methanol would likely result

\*Author to whom correspondence should be addressed.

in methanol (the polar molecule) being relatively hot and benzene (nonpolar) being relatively cold. Here, the role of the nanopore is to create a high-density adsorbed phase, and to facilitate conversion of rotational excitation into center-of-mass motion of adsorbed molecules.

We have since become interested in exploring *diffusion* in MW-heated zeolite-guest systems, which is important for understanding reactions and separations in these nanopores.<sup>15</sup> Although the technologically relevant diffusion process involves non-equilibrium concentration gradients, here we focus on modeling self-diffusion, i.e., the stochastic motion of tagged particles in the absence of concentration gradients. Our present focus on self-diffusion is motivated by statistical considerations in molecular simulations: gathering sufficient statistics when modeling self-diffusion is much easier than that for gradient diffusion, because in the former case, each molecule provides independent statistics. Because this is the first-ever simulation study of diffusion in MW-heated zeolites, and the non-equilibrium nature of these MW simulations is already complex, we begin our study of diffusion by focusing on the simpler transport process, namely self-diffusion. In a forthcoming publication, we turn our attention to gradient diffusion in MW-heated zeolites. In what follows, we omit the prefix “self” for brevity, referring simply to diffusion and diffusivities.

A number of situations with varying complexities can be envisioned for MW-heated diffusion in zeolites; here we introduce a few possibilities. Perhaps the simplest case involves a MW-heated single-component adsorbed phase (A) in a zeolite (Z), with energy fluctuations controlled by temperatures  $T_A$  and  $T_Z$ , respectively. For a given loading, the simplest outcome involves the MW-heated diffusivity equaling the equilibrium diffusivity at temperature  $T_A$ . For a binary mixture of A and B adsorbed in a zeolite Z, with temperatures  $T_A$ ,  $T_B$  and  $T_Z$ , respectively, our previous simulation results suggest a picture with different components diffusing at different temperatures. In other words, we might expect that  $D_A = D_A^{\text{eq}}(T_A)$  and  $D_B = D_B^{\text{eq}}(T_B)$ , where the equilibrium diffusivities are taken from a multi-component system with the same loadings as in the MW-heated system. We test these notions in the present article by performing a variety of equilibrium and non-equilibrium simulations on benzene and methanol in de-aluminated Y (DAY) zeolite.

The situations above assume that a given adsorbed-phase component acts as if it were completely thermalized at its own MW-heated temperature. Another level of complexity can be appreciated by taking the classical statistical mechanics viewpoint, involving separate probability distributions for the position ( $\vec{r}$ ) and momentum ( $\vec{p}$ ) vectors of each adsorbate’s center-of-mass. For an equilibrium system at temperature  $T$ , the phase-space distribution is given by the product  $F_T(\vec{p})G_T(\vec{r})$ , where  $F_T(\vec{p})$  is the familiar Maxwell-Boltzmann distribution of momenta. For a MW-heated adsorbed phase, we consider the possibility that the phase-space distribution can become  $F_{T_1}(\vec{p})G_{T_2}(\vec{r})$ , i.e.,

the distributions over positions and momenta correspond to *different* effective temperatures. In our previous work, we have analyzed only the velocity distributions in MW-heated systems, because in this case, each molecule provides its own velocity statistics.<sup>14</sup> We found in MD simulations that, even for MW-heated systems, all velocity distributions remain Gaussian. As such, each molecule’s center-of-mass can be characterized by an effective temperature extracted from these Gaussians. We denote these temperatures as “kinetic temperatures” ( $T_K$ ), because of their connection with kinetic energy. It remains to be seen whether distributions over potential energies in MW-heated systems correspond to any temperature, and if so, if this “potential temperature” ( $T_V$ ) equals the kinetic temperature. We explore these issues in the present paper.

Equilibrium diffusion in zeolites is often composed of distinct cage-to-cage jumps. This idea has been demonstrated for diffusion in a variety of zeolite frameworks, including FAU,<sup>16</sup> LTA<sup>17</sup> and MFI.<sup>18</sup> The temperature dependence for cage-to-cage rate constants usually takes the form  $k = A(T) \exp(-E_a/RT)$ , where  $A(T)$  is an effective attempt frequency, which depends weakly on temperature, and  $\exp(-E_a/RT)$  is the Arrhenius-Boltzmann factor, which is clearly very sensitive to temperature. We note that the Arrhenius factor arises from sampling potential energy distributions, while the attempt frequency is largely determined by kinetic energy distributions. Armed with these facts and the ideas above, we anticipate the possibility that the cage-to-cage rate constant in MW-heated systems may take the form:  $k_{\text{mw}} = A(T_K) \exp(-E_a/RT_V)$ , i.e., the attempt frequency and Arrhenius factor may be controlled by different temperatures. We investigate such ideas below.

By making appropriate comparisons between equilibrium and non-equilibrium MD simulations, we find below that MW-heated potential energy distributions can be associated with temperatures. However, these potential temperatures are consistently higher than kinetic ones. This finding has important consequences for MW-heated diffusion in zeolites, which we discuss below. The remainder of this article is organized as follows: in Sec. 2, we discuss the methods used in our MD simulations of benzene and methanol in de-aluminated Y zeolite. In Sec. 3, we give the results and discussion, and in Sec. IV, we offer concluding remarks.

## 2. METHODOLOGY

Here we outline the methods required to investigate MW-driven diffusion of methanol and benzene in de-aluminated Y (DAY) zeolite. We describe the atomistic models of zeolite and guests, specify the potential energy function, and discuss the MD simulations and data analyses. Much of this has been detailed in our previous publications;<sup>13, 14</sup> here we outline the salient details to give a flavor of the computations.

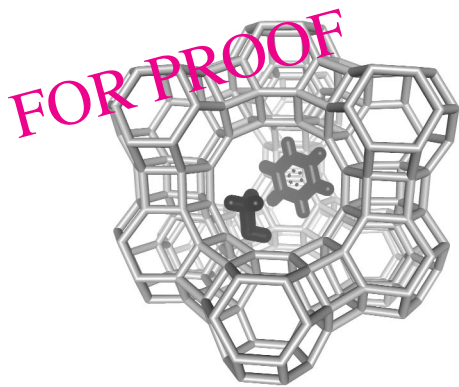


**Figure 1.** Schematic of DAY zeolite with adsorbed methanol and benzene.

## 2.1. Zeolite-Guest Models

DAY zeolite is the siliceous analog of zeolites faujasite, X and Y, all with the FAU framework topology.<sup>10, 19</sup> The schematic structure of this framework is shown in Fig. 1. We modeled diffusion in DAY because this material was studied in the MW-heated experiments of Turner et al.,<sup>9</sup> and because diffusion in the relatively large cages of DAY is sufficiently rapid to be sampled by MD. DAY contains roughly spherical cages that are connected through tetrahedral coordination. As such, each cage is connected to four others through so-called 12-ring windows with diameters of ca. 7.5 Å. This window size is large enough to allow sorption and diffusion of relatively large molecules such as xylenes and other branched hydrocarbons.<sup>20</sup> Each DAY cage can hold several molecules of benzene and/or methanol. As discussed above, the DAY nanopore helps to produce a high-density adsorbed phase, and facilitates the conversion of rotational to translational excitation.

The unit cell of DAY is face-centered cubic with 192 Si atoms and 384 O atoms. This unit cell forms 8 cages within a cubic lattice parameter of 24.3 Å.<sup>19</sup> All simulations reported below used the unit cell as the basic simulation cell. These simulations were performed by fixing the cell volume, the numbers of each type of particle, and by fixing the zeolite framework atoms during diffusion simulations for computational efficiency. Keeping the DAY frame fixed during diffusion simulations is a reasonable approximation because of DAY's relatively large windows. Most of the simulations discussed below include 8 or 16 molecules per DAY unit cell, i.e., 1 or 2 molecules per cage.

## 2.2. Potential Energy Surface

The potential energy has the form:

$$V = V_Z + V_G + V_{ZG} + V_{GG} \quad (1)$$

where  $V_Z$ ,  $V_G$ ,  $V_{ZG}$  and  $V_{GG}$  are the potential energy functions representing zeolite flexibility, guest flexibility, zeolite-guest interactions and guest-guest intermolecular

interactions, respectively. With the exception of  $V_G$ , which is taken to be a valence-bond function, each of the potential functions involves electrostatic energies and short-range interactions. The electrostatic contribution is calculated using Ewald sums over fixed partial charges. The fixed point charge approximation is reasonable in the present context because of the large frequency mismatch between typical MW frequencies and frequencies associated with electronic polarizabilities of oxide materials. Regarding short-range potentials,  $V_Z$  contains the Buckingham (exp-6) potential, while  $V_{ZG}$  and  $V_{GG}$  contain the Lennard-Jones (12-6) potential. Details about the potential functions and parameters can be found in Ref. 14 and references therein.

The electric charge distribution not only plays an important role in determining potential energies in our zeolite-guest model, but also controls energy transfer from the MW field (*vide infra*).<sup>21</sup> All partial charges are taken from previous publications. The benzene charges were extracted from MNDO calculations of Bull et al.;<sup>22, 23</sup> the zeolite charges were fitted to infrared (IR) spectra by analyzing dipole autocorrelation functions;<sup>24</sup> and methanol charges were obtained by performing electronic structure calculations.<sup>14</sup>

## 2.3. MD Simulations

All MD simulations were performed with our program Dizzy.<sup>25</sup> Periodic boundary conditions were enforced via the minimum image convention.<sup>26</sup> Short-range interactions were cut-off and shifted at 12 Å. All MD simulations were initiated from energy-minimized zeoliteguest structures, which were obtained by our simulated annealing procedure called MDDocker.<sup>23, 27</sup> Such an initial condition allows us to target particular temperatures with or without a thermostat (*vide infra*) by exploiting the nearly harmonic nature of zeolite-guest systems. Indeed, nearly half the initial kinetic energy pools into potential energy (on average) during the equilibration period. We employed the velocity Verlet algorithm to integrate Newton's equations with a time step of 1 fs. Total simulation times were at least 0.3 ns for sorption simulations and at least 10 ns for diffusion simulations.

To simulate the dynamics of zeolite-guest systems driven by MWs, we make the classical dipole approximation for the interaction between matter and light. That is, the zeoliteguest Hamiltonian is augmented by  $-\vec{\mu}_t \cdot \vec{E}_t$ , where  $\vec{\mu}_t$  is the time-dependent zeolite-guest dipole moment and  $\vec{E}_t$  is the MW electric field. We assume that the MW field points along the  $z$ -axis, and is homogeneous in space, because its wavelength is huge compared to typical MD length scales. We consider a monochromatic electric field of the form  $\vec{E}_t = E \cdot \hat{z} \cdot \cos(\omega t)$ , where  $E$  is the MW field strength and  $\omega$  is the MW frequency. Consistent with our previous MW simulations,<sup>13, 14</sup> we approximate that the zeolite-guest dipole moment can be represented by fixed point charges on all atoms in the system.

Given these approximations, Hamilton's equations of motion become:

$$\frac{d\vec{r}_i}{dt} = \frac{\vec{p}_i}{m_i} \quad \frac{d\vec{p}_i}{dt} = -\frac{\partial V}{\partial \vec{r}_i} + q_i \cdot \vec{E}_r, \quad (2)$$

where  $\vec{r}_i$  and  $\vec{p}_i$  are the three-dimensional position and momentum of particle  $i$ , respectively,  $m_i$  and  $q_i$  are its mass and charge, and  $V = V(\vec{r}_1, \vec{r}_2, \dots, \vec{r}_N)$  is the zeolite-guest potential energy function described above. The additional electrostatic force in Eq. (2), namely  $q_i \cdot \vec{E}_r$ , attempts to push charged particles to the left or right along the  $z$ -axis, depending upon the sign of the charge and the phase of the electric field. Such forces can excite vibrations of zeolite atoms and can excite external vibrations and librations of guest molecules in zeolites. The field strength was varied from 0.5 to 2.5 V/Å to obtain different steady-state temperatures. We set  $\omega$  to a value that falls in the blue end of the MW spectrum:  $9.4 \times 10^{11} \text{ s}^{-1}$ .<sup>13, 14</sup>

Steady-state conditions are produced by introducing a thermostat to simulate the cooling that occurs when carrier gas particles (such as He) collide with MW-heated zeolite-guest particles on the inflow side of the reactor.<sup>8, 9</sup> We applied the Andersen thermostat, which replaces the three-dimensional velocities of randomly selected atoms at random times with those from appropriate Maxwell-Boltzmann distributions.<sup>28</sup> The velocity replacements of different particles are assumed to be uncorrelated, occurring at random times chosen from a Poisson distribution. We implemented Andersen's thermostat in Dizzy by specifying two parameters in addition to the target temperature:  $\tau$ , the average time between velocity replacements, and  $n$ , the number of particles influenced at each replacement. Therefore, the Andersen thermostat allows explicit control over the number of particles influenced at each time step. In practice, the ratio of Andersen parameters,  $\tau/n$ , is sufficient to distinguish one Andersen thermostat from another. We have shown previously that the Andersen thermostat yields steady states that are reasonably robust to changes in thermostat parameters.<sup>13, 14</sup> As in our previous work, we set  $\tau/n$  to 10 fs per particle.

As discussed in the Introduction, we investigate below MW-heated energy distributions in some detail for methanol in DAY. We extract kinetic temperatures ( $T_K$ ) for methanol center-of-mass motion by properly normalizing its kinetic energy. We also construct histograms of the potential energies  $V_{ZG}$ ,  $V_{GG}$  and  $V_G$  using data from equilibrium and MW-heated MD runs. In what follows, we focus on the host-guest interaction,  $V_{ZG}$ , which is the most important for controlling sorption and diffusion in nanopores. The qualitative conclusions we draw regarding  $V_{ZG}$  were found to apply to the other potential energies as well. Below we find that equilibrium and MW-heated histograms of  $V_{ZG}$  are qualitatively the same: namely, asymmetric unimodal distributions. We define the temperature of a MW-heated  $V_{ZG}$  distribution from its first moment. That is, we

compute  $\langle V_{ZG} \rangle_{mw}$  from MW-heated steady states and also  $\langle V_{ZG} \rangle_T$  from equilibrium MD. The value of temperature for which  $\langle V_{ZG} \rangle_{mw} = \langle V_{ZG} \rangle_T$  is defined as the potential temperature,  $T_V$ , of a MW-heated system. Below we compare kinetic and potential temperatures of MW-heated systems to determine their correspondence, if any.

Mean-square displacements (MSDs) were calculated for each molecule with a time average according to:

$$\langle |\vec{r}(t) - \vec{r}(0)|^2 \rangle \approx \frac{1}{N_{MD} - n} \sum_{i=1}^{N_{MD}-n} |\vec{r}(i+n) - \vec{r}(i)|^2 \quad (3)$$

where  $N_{MD}$  is the number of MD steps. Diffusion coefficients were extracted from long-time linear slopes of MSDs (divided by 6), being careful to ensure that these simulations accessed diffusional length and time scales. In all cases, linear MSDs were obtained for lengths well beyond the cage-to-cage length of ca. 10 Å.

To avoid unphysical energy drifts during MW-heated MD simulations, we equilibrated the system for 5 ps before applying the MW field. The thermostat temperature was set to 200 K when targeting steady-state kinetic temperatures in the range 200–300 K and set to 300 K when MW-heating above 300 K.

### 3. RESULTS AND DISCUSSION

We begin by addressing the question of whether potential temperatures of MW-heated systems are meaningful, and if so, how they compare with kinetic temperatures. Figure 2 shows histograms of the host-guest potential energy,  $V_{ZG}$ , arising from equilibrium MD (EMD) of 16 methanols in flexible DAY at  $T = 604$  and 844 K. Temperature fluctuations during these EMD runs are typically  $\pm 10$  K. Also shown is the  $V_{ZG}$  histogram from MW-heated MD (MWMD) on the same system, thermostatted at  $T = 300$  K with a MW field strength of  $E = 2.0$  V/Å. As can readily be seen in Fig. 2,  $V_{ZG}$  histograms from EMD at 604 K and

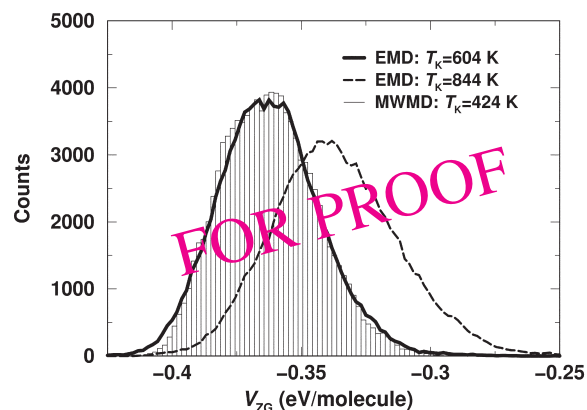


**Figure 2.** Histograms of host-guest potential energy in equilibrium and MW-heated methanol/DAY systems. The histogram shown as a bar graph is from MWMD.

MWMD at  $E = 2.0 \text{ V/\AA}$  are virtually identical, suggesting that MW-heated potential energy distributions can be characterized by effective temperatures,  $T_V$ . (It remains to be seen whether this holds for zeolite-guest systems with several distinct types of binding sites.) Figure 2 suggests that  $T_V = 604 \text{ K}$  for MWMD at  $E = 2.0 \text{ V/\AA}$ . We note that the kinetic temperature for this MWMD simulation is  $T_K = 424 \text{ K}$ , significantly below  $T_V$ . It is interesting to explore whether the inequality  $T_V > T_K$  holds for other MW field strengths as well.

To address this question, we could proceed by repeating the histogram comparisons shown in Fig. 2, but for different MW field strengths. However, we have found by thorough inspection of EMD and MWMD results (data not shown) that the  $V_{ZG}$  distributions are essentially identical when  $\langle V_{ZG} \rangle_{mw} = \langle V_{ZG} \rangle_T$ , i.e., the first moments being equal is sufficient for these distributions to be the same. We can thus address this question by comparing averages of  $V_{ZG}$  from EMD at various temperatures, and MWMD at various field strengths. In Fig. 3, we show  $\langle V_{ZG} \rangle_T$  from EMD for 16 methanols in flexible DAY at temperatures in the range 300–850 K. EMD results with and without the Andersen thermostat are shown in Fig. 3. Their agreement indicates that energy transfer with DAY's framework vibrations is sufficient to thermalize the system, and that these EMD results are well-equilibrated to the canonical ensemble. Also shown in Fig. 3 is  $\langle V_{ZG} \rangle_{mw}$  from MWMD on the same system at field strengths  $E = 0.5, 1.0, 1.5, 2.0$  and  $2.5 \text{ V/\AA}$ . These MWMD simulations exhibit steady-state kinetic temperatures in the range 333–440 K, which are used as the abscissas in Fig. 3. Figure 3 clearly shows that these MW-heated systems give  $\langle V_{ZG} \rangle$  values higher than expected from the kinetic temperatures for all field strengths studied.

For each MWMD simulation, we determine a potential temperature by finding the equilibrium temperature whose  $\langle V_{ZG} \rangle_T$  equals the  $\langle V_{ZG} \rangle_{mw}$  value in question. For example, MWMD with the field strength  $E = 1.5 \text{ V/\AA}$  gives a kinetic temperature of 398 K and  $\langle V_{ZG} \rangle_{mw} = -0.37 \text{ eV/mol}$ .

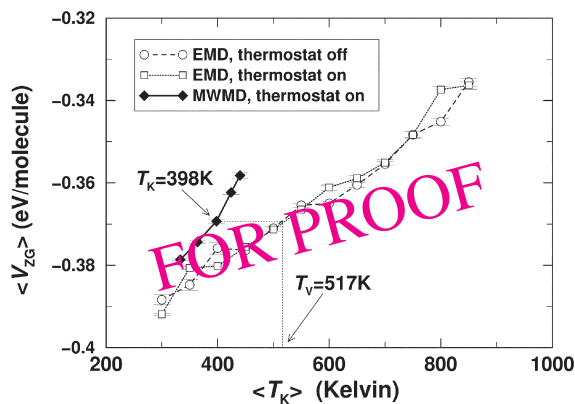


**Figure 3.** Comparing  $\langle V_{ZG} \rangle$  from equilibrium MD (EMD) and MW-heated MD (MWMD) for 16 methanols in flexible DAY. MWMD run with field strengths  $E = 0.5, 1.0, 1.5, 2.0$  and  $2.5 \text{ V/\AA}$ , giving the steady-state kinetic temperatures shown in the x-axis.

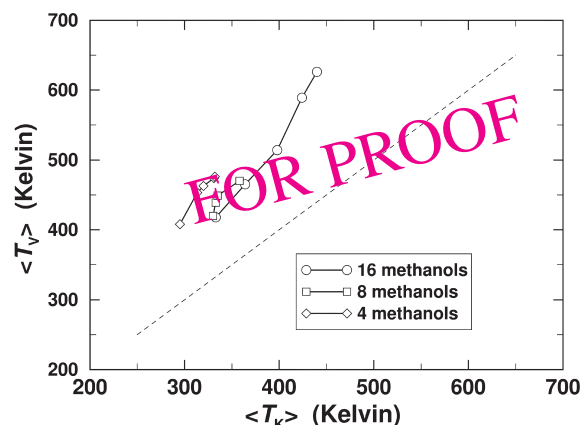


**Figure 4.** Comparison between potential and kinetic temperatures of MW-heated methanol in DAY zeolite, for various methanol loadings. MW field strengths in the range  $0.5$ – $2.5 \text{ V/\AA}$ .

ecule (see Fig. 3). An equilibrium system at  $T = 517 \text{ K}$  would give the same average host-guest energy, suggesting  $T_V = 517 \text{ K}$  for this MW field strength. Repeating this analysis for several field strengths gives MW-heated potential temperatures vs. kinetic temperatures. These are shown in Fig. 4 for loadings of 4, 8 and 16 methanols in flexible DAY. The dashed line shows the equilibrium result, namely  $T_K = T_V$ . In all cases, we find that  $T_V$  is significantly higher than  $T_K$ . Thus, the kinetic temperature alone should fail to predict sorption and diffusion behavior in MW-heated zeolite-guest systems.

All the simulations and analyses presented herein have focused on methanol in DAY. We have performed the same investigation on benzene in DAY (data not shown). In contrast to the results for methanol in DAY, MW-heated benzene in DAY does not exhibit any statistically significant difference in kinetic and potential temperatures. In fact, benzene in DAY exhibits little MW-heating, presumably because benzene lacks a permanent dipole moment.

The results in Fig. 4 suggest that MW-heated diffusivities will exceed equilibrium diffusivities at the same kinetic temperature, because the hotter potential energy distributions in MW-heated molecules will allow them to traverse potential barriers more rapidly. To test this idea, we simulated diffusion of benzene and/or methanol in DAY at equilibrium and under MW-heating. The results are shown in Fig. 5 plotted against the kinetic temperatures from EMD and MWMD simulations. Figure 5 shows results in the temperature range 300–450 K for six distinct systems in DAY: EMD of 8 methanols, MWMD of 8 methanols, EMD of 8 benzenes, MWMD of 8 benzenes, EMD of 8 methanols and 8 benzenes, and MWMD of 8 methanols and 8 benzenes.

We begin by analyzing the equilibrium diffusion results. Single-component methanol EMD diffusivities fall in the range  $4.9$ – $10.3 \times 10^{-5} \text{ cm}^2 \text{ s}^{-1}$ , while those for benzene fall in the range  $0.060$ – $2.5 \times 10^{-5} \text{ cm}^2 \text{ s}^{-1}$ . Our simula-

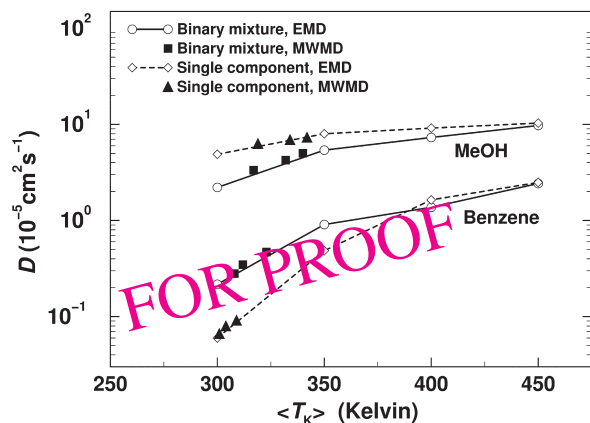


**Figure 5.** Self-diffusion constants of single components (8 methanols or 8 benzenes) and binary mixtures (8 methanols and 8 benzenes) in DAY zeolite from equilibrium MD (EMD) and MW-heated MD (MWMD).

tions portray benzene diffusion in DAY as slower than methanol motion, and more sensitive to temperature. As such, benzene diffusion is predicted to be a more activated process than is methanol diffusion. Indeed, the apparent activation energies extracted from single-component EMD are  $E_a = 3.7 \text{ kJ mol}^{-1}$  and  $E_a = 12.5 \text{ kJ mol}^{-1}$  for methanol and benzene in DAY, respectively. Considering that thermal energy ( $RT$ ) is  $2.49\text{--}3.74 \text{ kJ mol}^{-1}$  in the temperature range 300–450 K, benzene motion requires much more activation than does methanol diffusion. Experimental activation energies for benzene diffusion in DAY range from  $8\text{--}10 \text{ kJ mol}^{-1}$ ,<sup>22, 29</sup> in reasonable agreement with our simulated value. We are unaware of such experimental data for methanol in DAY. There are likely many factors contributing to these results, including the simple fact that benzene fits more tightly in DAY's 12-ring window than does methanol.

For the equilibrium binary mixture in DAY, the diffusivities fall in the ranges  $2.2\text{--}9.7 \times 10^{-5} \text{ cm}^2 \text{ s}^{-1}$  and  $0.21\text{--}2.4 \times 10^{-5} \text{ cm}^2 \text{ s}^{-1}$  for methanol and benzene, respectively. At the highest temperature (450 K), the single-component and binary-mixture diffusivities are essentially the same. However, at the lowest temperature (300 K), forming the mixture slows methanol diffusion by a factor of over 2 and speeds up benzene motion by a factor of 3.5. Benzene slowing methanol is no surprise, but methanol simultaneously speeding up benzene is interesting. This might arise from methanol competing for benzene's favorite adsorption sites within DAY.

Now we turn to the MW-heated diffusion results in Fig. 5. Single-component diffusivities for MW-heated methanol and benzene in DAY are shown for MW field strengths  $E = 0.5, 1.0$  and  $1.5 \text{ V/\AA}$ , all thermostatted at  $T = 300 \text{ K}$ . Methanol exhibits MW heating to kinetic temperatures of  $T_K = 319, 334$  and  $342 \text{ K}$ , respectively. When plotted against these kinetic temperatures, the MW-heated diffusivities for methanol fall right on the equilibrium line. This is surprising in light of our findings above

regarding potential temperatures consistently exceeding kinetic temperatures. However, these results for MW-heated methanol begin to make sense when we realize that in this temperature regime, methanol diffusion is not strongly activated, and hence is less sensitive to potential energy distributions (more on this below). Single-component benzene exhibits MW heating to only 301 K, 304 K and 309 K, respectively. This is consistent with benzene's lack of a permanent dipole moment. The MW-heated diffusivities of single-component benzene in Fig. 5 are nearly the same as benzene's equilibrium results at 300 K, indicating that MW heating has little effect on benzene's diffusion in DAY zeolite.

Perhaps the most technologically important simulation involves the multi-component MW-heated diffusion system in Fig. 5. Even though benzene by itself does not exhibit much MW heating, when co-adsorbed with methanol, benzene can heat through energy transfer from MW-excited methanol. Indeed, our results in Fig. 5 show that co-adsorbed benzene exhibits MW heating to 308 K, 312 K and 323 K, i.e., slightly higher temperatures than for single-component benzene. On the other hand, co-adsorbed methanol's MW-heated temperatures are essentially unchanged from their single-component values. The diffusivities obtained in this case are consistent with the notion of "different components diffusing with different temperatures," as suggested in the Introduction.

All diffusion becomes activated at sufficiently low temperatures. As such, by reducing the thermostat temperature, we can put methanol diffusion in DAY in its activated regime, becoming more sensitive to potential energy distributions and possibly MW heating. Figure 6 shows EMD and MWMD results for methanol down to lower temperatures than were considered in Fig. 5. The low-temperature MWMD results were obtained using a 200 K thermostat. We see a striking result in Fig. 6. At higher temperatures, we find that MWMD and EMD agree when plotted against kinetic temperature, as seen in Fig. 5. However, at lower

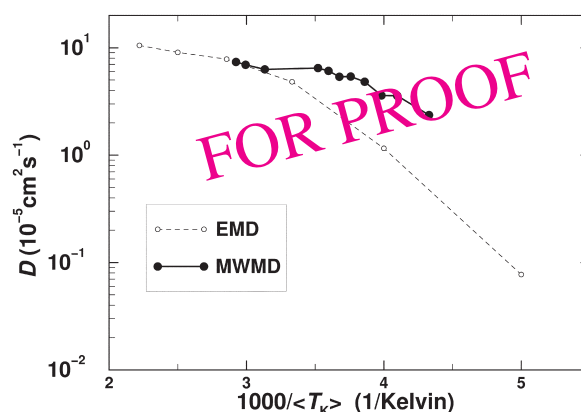


**Figure 6.** Diffusion constants for methanol in DAY zeolite from EMD and MWMD, showing that kinetic temperatures underestimate MW-heated diffusivities when diffusion is activated.

temperatures, we find that MWMD diffusivities consistently exceed EMD diffusivities at the same kinetic temperature, presumably because the MW-heated potential distributions enable more facile barrier crossing. This result shows that in general, MW-heated diffusion is more complicated than simply “different components diffusing at different temperatures.” Instead, we advocate the picture involving “different components diffusing at different kinetic and potential temperatures.”

#### 4. CONCLUDING REMARKS

We have performed equilibrium molecular dynamics (EMD) and microwave-heated molecular dynamics (MWMD) simulations to explore how MW heating influences self-diffusion in zeolite nanopores. We have applied these simulations to methanol (polar) and/or benzene (nonpolar) in DAY zeolite. In general, we find that even under the non-equilibrium conditions of MW heating, center-of-mass motions can be associated with effective temperatures. However, we find that the temperatures controlling kinetic and potential energy distributions are not generally the same in MW-heated systems, with potential temperatures generally exceeding kinetic ones.

This finding has a consequence for understanding MW-heated diffusion in zeolite nanopores. In particular, when temperatures are sufficiently high that diffusion is not strongly activated, MW-heated diffusivities are equal to equilibrium diffusivities at the same kinetic temperature. On the other hand, when diffusion becomes more strongly activated at lower temperatures, MWMD diffusivities consistently exceed EMD diffusivities at the same kinetic temperature, because the MW-heated potential distributions enable more facile barrier crossing. This result shows that in general, MW-heated diffusion is more complicated than simply “different components diffusing at different temperatures.” Instead, we advocate the picture involving “different components diffusing at different kinetic and potential temperatures.”

Strictly speaking, the conclusions from this study pertain only to MW-heating of small molecules in dry silica zeolites. However, it is intriguing to consider these ideas applied to very different MW-heated systems. For example, MW heating in zeolite synthesis can have profound effects, speeding up reactions from hours or days to minutes, and in some cases, improving the crystallinity of resulting materials. For such systems, we imagine that MW heating can produce broad potential energy distributions, allowing for the facile bond breaking and making required for zeolite crystallization. Many more experiments and simulations are required to firmly establish the role of microwaves in zeolite nanopores.

**Acknowledgments:** We thank Prof. Curt Conner and Prof. Bret Jackson for enlightening discussions regarding microwaves, zeolites and thermostats. We are grateful for generous funding from the UMass Amherst Department of Chemistry for computational resources, from the UMass Amherst Faculty Research Grant program, and from the National Science Foundation Nanoscale Interdisciplinary Research Team program (grant number CTS-0304217).

#### References and Notes

1. S. M. Auerbach, K. A. Carrado, and P. K. Dutta, editors, *Handbook of Zeolite Science and Technology*, Marcel Dekker, Inc., New York, (2003).
2. C. S. Cundy, *Collect. Czech. Chem. Commun.* 63, 1699 (1998).
3. S. Mintova, S. Mo, and T. Bein, *Chem. Mater.* 10, 4030 (1998).
4. K. J. Rao, B. Vaidhyanathan, M. Ganguli, and P. A. Ramakrishnan, *Chem. Mater.* 11, 882 (1999).
5. J. M. Lopes, F. N. Serralha, C. Costa, F. Lemos, and R. Ribeiro, *Catal. Lett.* 53, 103 (1998).
6. M. Hajek, *Collect. Czech. Chem. Commun.* 62, 347 (1996).
7. C. Marun, L. D. Conde, and S. L. Suib, *J. Phys. Chem. A* 103, 4332 (1999).
8. S. Kobayashi, Y.-K. Kim, C. Kenmizaki, S. Kushiyama, and K. Mizuno, *Chem. Lett.* 9, 769 (1996).
9. M. D. Turner, R. L. Laurence, W. C. Conner, and K. S. Yngvesson, *AIChE J.* 46, 758 (2000).
10. C. Baerlocher, W. M. Meier, and D. H. Olson, *Atlas of Zeolite Framework Types*, Elsevier, Amsterdam, fifth edition, 2001, <http://www.iza-structure.org/databases>.
11. D. A. C. Stuerge and P. Gaillard, *J. Microwave Power Electromagn. Energy* 31, 87 (1996).
12. D. A. C. Stuerge and P. Gaillard, *J. Microwave Power Electromagn. Energy* 31, 101 (1996).
13. C. Blanco and S. M. Auerbach, *J. Am. Chem. Soc.* 124, 6250 (2002).
14. C. Blanco and S. M. Auerbach, *J. Phys. Chem. B* 107, 2490 (2003).
15. J. Kärger, S. Vasenkov, and S. M. Auerbach, *Diffusion in Zeolites, in Handbook of Zeolite Science and Technology*, edited by S. M. Auerbach, K. A. Carrado, and P. K. Dutta, pp. 341–422, Marcel Dekker, Inc., New York, 2003.
16. S. M. Auerbach and H. I. Metiu, *J. Chem. Phys.* 105, 3753 (1996).
17. A. Schüring, S. M. Auerbach, S. Fritzsche, and R. Haberlandt, *J. Chem. Phys.* 116, 10890 (2002).
18. S. C. Turaga and S. M. Auerbach, *J. Chem. Phys.* 118, 6512 (2003).
19. J. A. Hriljac, M. M. Eddy, A. K. Cheetham, J. A. Donohue, and G. J. Ray, *J. Solid State Chem.* 106, 66 (1993).
20. C. M. Freeman et al., *ACS Sym. Ser.* 589, 326 (1995), and references therein.
21. J. D. Jackson, *Classical Electrodynamics*, Wiley, New York, 1975.
22. L. M. Bull, N. J. Henson, A. K. Cheetham, J. M. Newsam, and S. J. Heyes, *J. Phys. Chem.* 97, 11776 (1993).
23. S. M. Auerbach, N. J. Henson, A. K. Cheetham, and H. I. Metiu, *J. Phys. Chem.* 99, 10600 (1995).
24. E. Jaramillo and S. M. Auerbach, *J. Phys. Chem. B* 103, 9589 (1999).
25. N. J. Henson, *Ph.D. thesis*, Oxford University, 1996.
26. M. F. Allen and D. J. Tildesley, *Computer Simulation of Liquids*, Oxford Science Publications, Oxford, (1987).
27. E. Jaramillo, C. P. Grey, and S. M. Auerbach, *J. Phys. Chem. B* 105, 12319 (2001).
28. H. C. Andersen, *J. Chem. Phys.* 72, 2384 (1980).
29. Y. H. Chen and L. P. Hwang, *J. Phys. Chem. B* 103, 5070 (1999).

(Received: . Revised/Accepted: )